Proc. Natl. Acad. Sci. USA
Vol. 95, pp. 12940–12943, October 1998
Biophysics

High-frequency, spin-label EPR of nonaxial lipid ordering and motion in cholesterol-containing membranes

BETTY J. GAFFNEY* AND DEREK MARSH†‡

*National High Magnetic Field Laboratory and Department of Biological Science, Florida State University, 1800 E. Paul Dirac Drive, Tallahassee, FL 32310; and †Abteilung Spektroskopie, Max-Planck-Institut für biophysikalische Chemie, Am Fassberg 11, D-37077 Göttingen, Germany

Edited by Harden M. McConnell, Stanford University, Stanford, CA, and approved August 28, 1998 (received for review May 22, 1998)

ABSTRACT **The EPR spectra of spin-labeled lipid chains in fully hydrated bilayer membranes of dimyristoyl phosphatidylcholine containing 40 mol % of cholesterol have been studied in the liquid-ordered phase at a microwave radiation frequency of 94 GHz. At such high field strengths, the spectra should be optimally sensitive to lateral chain ordering that is expected in the formation of in-plane domains. The high-field EPR spectra from random dispersions of the cholesterol-containing membranes display very little axial averaging of the nitroxide g-tensor anisotropy for lipids spin labeled toward the carboxyl end of the *sn*-2 chain (down to the 8-C atom). For these positions of labeling, anisotropic ^{14}N-hyperfine splittings are resolved in the g_{zz} and g_{yy} regions of the nonaxial EPR spectra. For positions of labeling further down the lipid chain, toward the terminal methyl group, the axial averaging of the spectral features systematically increases and is complete at the 14-C atom position. Concomitantly, the time-averaged $\langle A_{zz} \rangle$ element of the ^{14}N-hyperfine tensor decreases, indicating that the axial rotation at the terminal methyl end of the chains arises from correlated torsional motions about the bonds of the chain backbone, the dynamics of which also give rise to a differential line broadening of the ^{14}N-hyperfine manifolds in the g_{zz} region of the spectrum. These results provide an indication of the way in which lateral ordering of lipid chains in membranes is induced by cholesterol.**

The formation of in-plane domains in biological membranes is expected to be accompanied and partly driven by lateral ordering of lipid chains (1, 2). Hence, physical methods for detecting lateral ordering are of direct relevance to this crucial aspect of membrane biology. At the 9-GHz microwave frequency and 0.35 T field of conventional EPR spectroscopy with nitroxide spin labels, anisotropic contributions to the spectra are dominated by nitrogen hyperfine structure, the anisotropy of which is dipolar in origin and is therefore of axial symmetry. At higher operating frequencies, however, the nitroxide Zeeman interaction exceeds that of the nitrogen hyperfine interactions (3–6). As a result of the nonaxial g-tensor of nitroxide radicals, high-frequency EPR spectroscopy renders the spectra of oxazolidine-*N*-oxyl spin-labeled lipid chains sensitive to ordering in the plane of the membrane and to the rate of rotation about the normal to this plane. Spin labeling then becomes particularly appropriate for studying the contribution of membrane in-plane motion to dynamic ordering of lipid assemblies in biological membranes. Of special current interest is the liquid-ordered phase of membranes containing a high content of cholesterol (7, 8). This is because this phase has been proposed to constitute detergent-insoluble domains that preferentially segregate specific membrane components and are the vehicles for sorting in cellular membrane traffic (9, 10).

In the present work, we have studied motion and ordering of spin-labeled lipid chains by using EPR spectroscopy at a microwave frequency of 94 GHz and a field strength of 3.35 T. This frequency is high enough to render the spectra responsive to in-plane motions, but low enough to leave the spectra sensitive to correlation times as long as 10^{-7} s. Phospholipids spin labeled at different positions on the acyl chains were incorporated in hydrated bilayer membranes that contain cholesterol at a level normally encountered in mammalian cell plasma membranes. The spectra of the spin-labeled lipids reveal restricted rotation about the membrane normal, the extent of which depends on the position of chain labeling, decreasing from the polar–apolar interface toward the center of the ordered-fluid membranes. These results on lateral ordering of the lipids are directly relevant to the proposed stabilization of in-plane membrane domains by cholesterol.

MATERIALS AND METHODS

Dimyristoyl phosphatidylcholine (Myr_2PtdCho) was obtained from Avanti Polar Lipids and myristic acid (MA) and cholesterol from Merck. Oxazolidine-*N*-oxyl spin-labeled stearic acids {*n*-(4,4-dimethyloxazolidine-*N*-oxyl)stearic acid; *n*-SASL} and the corresponding phosphatidylcholines spin labeled in the *sn*-2 chain {1-acyl-2-[*n*-(4,4-dimethyloxazolidine-*N*-oxyl)stearoyl]-*sn*-glycero-3-phosphocholine; *n*-PCSL} were synthesized as described in ref. 11. For these spin labels, the principal magnetic axes (*x, y, z*) of the nitroxide are oriented with *z* parallel and *x, y* perpendicular to the fully extended all-*trans* acyl chain, with *x* directed approximately along the N—O bond and *y* perpendicular to this (Fig. 1). Myr_2PtdCho, cholesterol (40 mol %), and 1 mol % *n*-PCSL spin label were codissolved in dichloromethane; the solvent was evaporated under a nitrogen gas stream, and the samples were dried under vacuum overnight. The dried lipid mixtures were then hydrated with an excess of distilled water at a concentration of 65 mg/ml. The resulting lipid dispersions were introduced into 0.5 mm i.d. quartz capillaries and then concentrated by centrifugation and the excess aqueous supernatant removed. For preparation of an anhydrous, near rigid-limit sample, dry Myr_2PtdCho and MA at a 1:2 mol ratio were mixed in the molten state at 55°C with 1 mol % 5-SASL spin label and introduced into 0.5 mm i.d. quartz capillaries. The capillaries were flame sealed.

EPR spectra were recorded at a microwave frequency of 94 GHz on a Bruker EleXsys heterodyne W-band EPR spectrometer (Bruker, Billerica, MA) with a TE_{01x}-mode cylindrical

The publication costs of this article were defrayed in part by page charge payment. This article must therefore be hereby marked "*advertisement*" in accordance with 18 U.S.C. §1734 solely to indicate this fact.

This paper was submitted directly (Track II) to the *Proceedings* office.
Abbreviations: *n*-SASL, *n*-(4,4-dimethyloxazolidine-*N*-oxyl)stearic acid; *n*-PCSL, 1-acyl-2-[*n*-(4,4-dimethyloxazolidine-*N*-oxyl)stearoyl]-*sn*-glycero-3-phosphocholine; Myr_2PtdCho, dimyristoyl phosphatidylcholine; MA, myristic acid.
‡To whom reprint requests should be addressed. e-mail: dmarsh@gwdg.de.

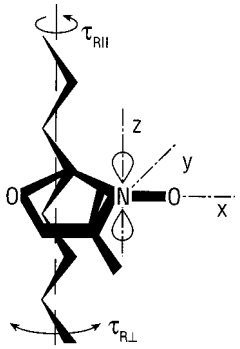

FIG. 1. Orientation of the magnetic axes (*x, y, z*) of the oxazolidine-*N*-oxyl spin-label group, relative to the all-*trans* axis (dashed line) of the acyl chain to which it is attached. Rotation about the chain axis ($\tau_{R//}$) and rotational flexing of the chain ($\tau_{R\perp}$) are indicated.

cavity resonator and a split-coil superconducting magnet. The intermediate frequency of 9.6 GHz was provided by a Gunn diode oscillator, with up-conversion by mixing with a phase-locked W-band Gunn source. Microwave power was in the range of 3−50 μW and loaded cavity Q was in the range 600-1200, depending on the sample. Field scans with room-temperature coils were of 30 or 60 mT width about a center magnetic field of 3.35 T. The Zeemann modulation frequency was 100 kHz, with peak-to-peak amplitudes of 0.05–0.2 mT. Sampling times were typically 40–160 ms, with 2–8 K points and filter time constants of 10–160 ms. Spectra were signal-averaged over 1–16 scans, depending on signal strength. Measurements were made at ambient temperature (22°C). For comparison purposes, spectra were also recorded at a frequency of 9 GHz on a Varian Century Line EPR spectrometer (Varian) equipped with field-frequency lock. Line positions were determined by fitting Lorentzian lineshapes to the absorption-like extrema, or from the point of maximum slope of the first-derivative-like features. Linewidths were determined from fitted absorption or first-derivative Lorentzian lineshapes, as appropriate.

RESULTS AND DISCUSSION

Rigid-Limit Spectrum. The 94-GHz EPR spectrum of a spin-labeled fatty acid (5-SASL) in a 1:2 mol/mol mixture of dimyristoyl phosphatidylcholine with MA is given in Fig. 2*A*. The room-temperature phase of this anhydrous mixture has a lamellar structure with hexagonally packed, nearly all-*trans* chains, which melts at a temperature of approximately 52°C (12). In the powder spectrum of the nonhydrated phase, the resonances from spin labels with the magnetic field parallel to the nitroxide *x*-, *y*-, and *z*-axes appear in distinct regions, from low to high field, respectively. The g_{zz}-, g_{yy}-, and g_{xx}-positions are centered at field strengths of 3.3576 T, 3.3516 T, and 3.3469 T, respectively. The ^{14}N-hyperfine splittings A_{zz} and A_{yy} are resolved in the g_{zz} and g_{yy} regions, respectively. Table 1 includes the nitroxide spin Hamiltonian parameters that are deduced from this spectrum. For comparison, the corresponding rigid-limit g-tensors determined at 250 GHz for 16-PCSL in a relatively apolar environment were (g_{xx}, g_{yy}, g_{zz}) = (2.00929, 2.00600, 2.00212) and (2.00926, 2.00593, 2.00212) in frozen hydrated bilayers of dipalmitoyl and palmitoyl-oleoyl phosphatidylcholines, respectively, at −150°C (4). The corresponding values of the ^{14}N-hyperfine tensor *z*-element were A_{zz} = 3.35 mT and 3.41 mT, respectively. There is reasonably good agreement between spin Hamiltonian parameters obtained in the present study and those from the earlier work; differences may be attributed largely to differences in environment of the spin label, in particular to the hexagonal ordering of the lipid chains in the fatty acid-containing system.

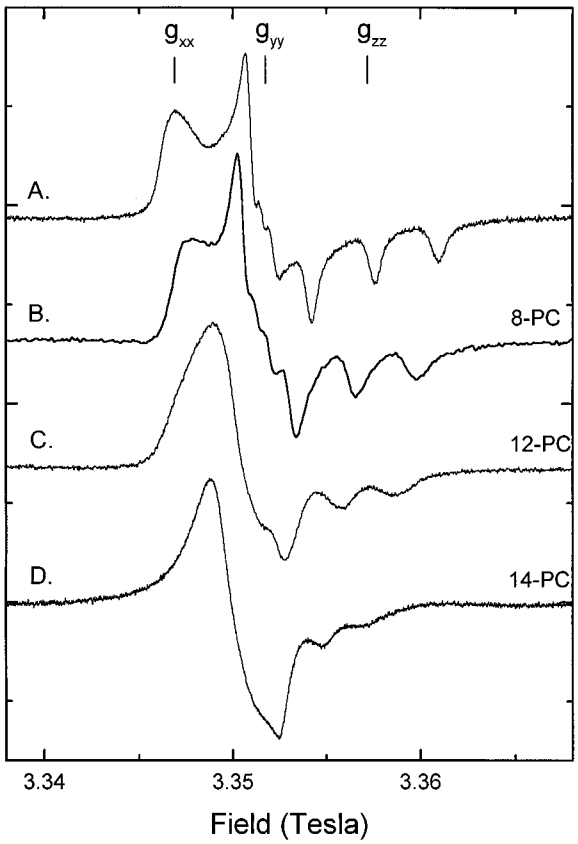

FIG. 2. EPR spectra at 94 GHz of lipids spin labeled in the fatty acid or acyl chain (n-SASL or *n*-PCSL, respectively). Spectrum A: 5-SASL in Myr_2PtdCho/MA 1:2 mol/mol anhydrous bilayers. Spectrum B: 8-PCSL in Myr_2PtdCho/cholesterol 3:2 mol/mol hydrated bilayer membranes. Spectrum C: 12-PCSL in Myr_2PtdCho/cholesterol 3:2 mol/mol. Spectrum D: 14-PCSL in Myr_2PtdCho/cholesterol 3:2 mol/mol. Spectra were recorded at slightly differing microwave frequencies and are aligned according to the $\langle g_{yy} \rangle$ values (Table 1) with the rigid-limit spectrum (spectrum A), which was recorded at a frequency of 94.1076 GHz. Total plot width = 30 mT.

Hydrated Membrane Spectra. The 94-GHz spectra of different positional isomers of the *n*-PCSL phosphatidylcholine spin label in fully hydrated bilayer membranes composed of dimyristoyl phosphatidylcholine with 40 mol % cholesterol are given in Fig. 2*B–D*. The cholesterol content of this model membrane is comparable to that found in cell plasma membranes and corresponds to the formation of a liquid-ordered phase (2, 13, 14). There is a systematic change in the spectral anisotropy with depth into the membrane on going from the 8-position spin label to the 14-position spin label in the chain. In the spectra of the 8-PCSL (and also 5-PCSL) spin label, with the nitroxide group toward the carboxyl end of the *sn*-2 acyl chain, the g_{xx}, g_{yy} and g_{zz} regions may be distinguished and the A_{zz} and A_{yy} ^{14}N-hyperfine splittings are resolved (see Fig. 2*B*), just as for the rigid-limit spectrum (Fig. 2*A*). Resolution of these features provides the basis for calculating an upper limit to the rate of phospholipid rotation about the chain long axis (see below). In the high-field spectrum of the 12-PCSL spin label, which is located further down the chain toward the methyl end, the anisotropy associated with the g_{xx} and g_{yy} tensor elements is reduced, as is the anisotropy characterized by the A_{zz} ^{14}N-hyperfine tensor element. The g_{xx} feature appears as an asymmetric shoulder at the low-field edge of the 12-PCSL spectrum, and the A_{zz} splitting of the high-field ^{14}N-hyperfine triplet is reduced (see Fig. 2*C*). At the position of the 14-PCSL spin label isomer, the x–y anisotropy is reduced to zero, producing a single first-derivative lineshape at the low-field

Table 1. Partially motionally averaged spin Hamiltonian parameters of spin-labeled n-PCSL in bilayer membranes of myr$_2$PtdCho/cholesterol 3:2 mol/mol, and rigid-limit parameters for spin-labeled stearic acid (5-SASL) in myr$_2$PtdCho/MA 1:2 mol/mol bilayers (microwave frequency, 94 GHz)

Spin label	$\langle g_{xx}\rangle$	$\langle g_{yy}\rangle$	$\langle g_{zz}\rangle$	$\langle A_{zz}\rangle$, mT	$\langle A_{yy}\rangle$, mT
		myr$_2$PtdCho-cholesterol			
5-PCSL	$2.0084 \pm 2{\cdot}10^{-4}$	$2.0064 \pm 1{\cdot}10^{-4}$	$2.0031 \pm 1{\cdot}10^{-4}$	3.36 ± 0.05	0.65 ± 0.14
8-PCSL	$2.00840 \pm 5{\cdot}10^{-5}$	$2.00634 \pm 5{\cdot}10^{-5}$	$2.00310 \pm 5{\cdot}10^{-5}$	3.18 ± 0.02	0.70 ± 0.02
12-PCSL	$2.0082 \pm 5{\cdot}10^{-4}$	$2.00696 \pm 5{\cdot}10^{-5}$	$2.00362 \pm 5{\cdot}10^{-5}$	2.88 ± 0.02	
14-PCSL	$2.00745 \pm 5{\cdot}10^{-5}$	$2.00745 \pm 5{\cdot}10^{-5}$	$2.00446 \pm 5{\cdot}10^{-5}$	2.19 ± 0.15	
		myr$_2$PtdCho/MA			
5-SASL	$2.00895 \pm 5{\cdot}10^{-5}$	$2.00617 \pm 5{\cdot}10^{-5}$	$2.00257 \pm 5{\cdot}10^{-5}$	3.37 ± 0.02	0.66 ± 0.02

side of the spectrum (see Fig. 2*D*). Concomitantly, the A_{zz} splitting of the high-field ^{14}N-hyperfine triplet is further reduced, corresponding to an increase in amplitude of motion about the chain axis. An increase in linewidth of each A_{zz} ^{14}N-hyperfine resonance accompanies the loss of x–y anisotropy.

Motional and Environmental Parameters. Models for the anisotropic motion reflected in the high-frequency EPR spectra of the spin-labeled phosphatidylcholines can be tested by using correlations among the motionally averaged parameters. These averaged spin Hamiltonian parameters from the different *n*-PCSL positional isomers in Myr$_2$PtdCho/cholesterol membranes are given in Table 1. The values reflect motion about the membrane normal, flexibility of the lipid chains, and polarity-dependent changes in the magnitudes of the tensor elements. In Fig. 3, the values of the partially averaged g-tensor elements, $\langle g_{ii}\rangle$, are plotted against the $\langle A_{zz}\rangle$ element of the ^{14}N-hyperfine tensor for the *n*-PCSL spin labels in fully hydrated Myr$_2$PtdCho/cholesterol 3:2 mol/mol membranes. The $\langle g_{zz}\rangle$ and $\langle A_{zz}\rangle$ tensor elements are correlated linearly because they reflect the same chain-flexing motions. The linear relation between $\langle g_{xx}\rangle$ or $\langle g_{yy}\rangle$ and $\langle A_{zz}\rangle$ indicates that rotation of the lipids around their long axis and flexing of the lipid chains are coupled. Cumulative segmental oscillations and possibly increased rates of oscillation down the lipid chain give a progressive increase in the degree of averaging about the membrane normal.

Polarity-dependent perturbations of the motional correlation are seen in comparison of the data for the 5-position labels in the hydrophobic Myr$_2$PtdCho/MA host crystals and the hydrated Myr$_2$PtdCho/cholesterol membranes in Fig. 3 (two rightmost points). Whereas the values for the $\langle g_{yy}\rangle$ and $\langle g_{zz}\rangle$ tensor elements differ between the two systems in the same direction, those for the $\langle g_{xx}\rangle$ element differ in the opposite direction. It is the $\langle g_{xx}\rangle$ element that exhibits the

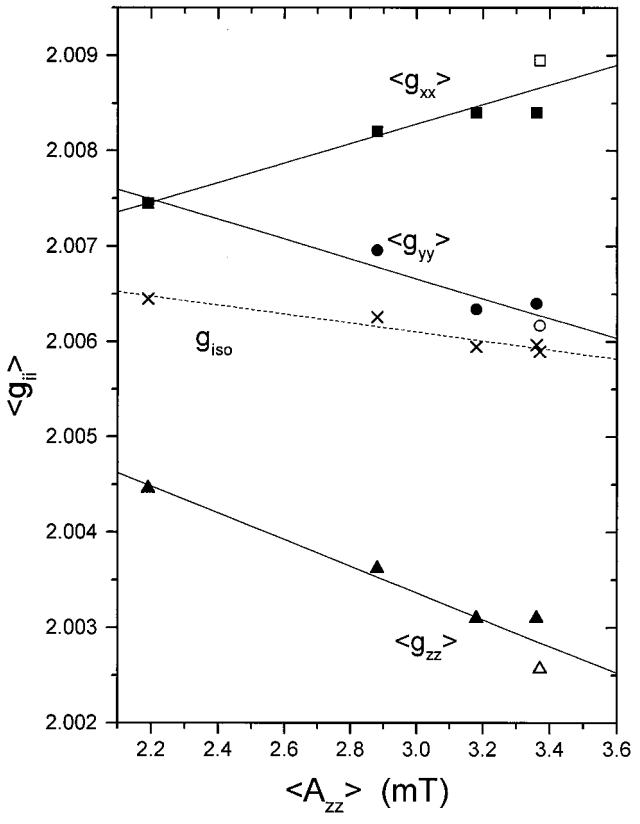

FIG. 3. Correlation of the partially motionally averaged g-tensor elements, $\langle g_{ii}\rangle$, with the $\langle A_{zz}\rangle$ element of the ^{14}N-hyperfine tensor for *n*-PCSL spin labels in hydrated Myr$_2$PtdCho/cholesterol 3:2 mol/mol membranes (filled symbols) and the rigid-limit values for 5-SASL in a Myr$_2$PtdCho/MA 1:2 mol/mol mixture (open symbols). The isotropic g-value, $g_{iso} = \mathrm{Tr}(\langle g_{ii}\rangle)$, is given by the crosses. With axial rotational averaging $\langle g_{yy}\rangle$ approaches $\langle g_{xx}\rangle$, rather than g_{iso}.

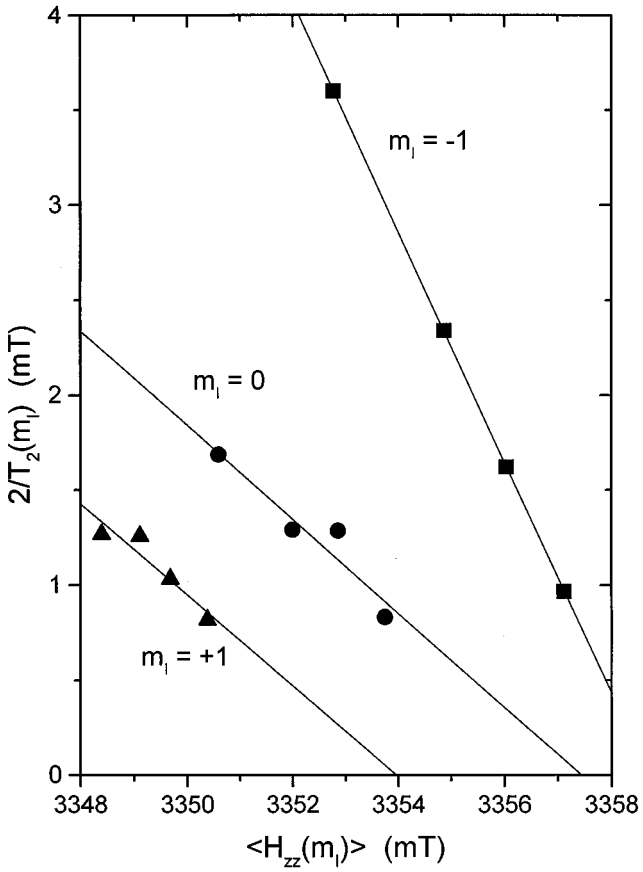

FIG. 4. Lorentzian full-widths, $2/T_2(m_I)$, of the g_{zz} hyperfine manifolds ($m_I = +1,0,-1$) as a function of resonance position, $\langle H_{zz}(m_I)\rangle$, for the different degrees of spectral shift of the various spin-label positional isomers.

major polarity dependence (4, 5), and the correlation with the difference in $\langle A_{zz} \rangle$ between the anhydrous sample and the hydrated membrane is exactly that expected for the relative polarities. An estimate of the polarity effect on the absolute value of g_{xx} for the environment of the 14-PCSL spin label can be made by assuming that the nonaveraged g_{yy} element (that is not very polarity-dependent) is equal to the rigid-limit value. The resulting value for 14-PCSL is $g_{xx} = 2\langle g_{xx} \rangle - g_{yy} = 2.0087$. This value implies an environment for 14-PCSL that is more apolar than that of 8-PCSL in the hydrated membranes, but less apolar than that in the anhydrous sample containing 5-SASL. It would be difficult to make such a polarity estimate from the 9-GHz EPR spectra for this system, because motional and polarity effects cannot be uncoupled in the latter case.

Chain Dynamics. The g_{xx} and g_{yy} features of an oxazolidine-*N*-oxyl chain-labeled lipid spectrum will be averaged if the frequency of rotation about the molecular long axis is fast compared with $(g_{xx}\text{-}g_{yy})\beta_e B_o/\hbar \approx 8 \times 10^8\ s^{-1}$ (at 3.5 T) (see Fig. 1). In the absence of complete x–y averaging, it is the magnitude of the detectable shift in value of the averaged tensor elements, from the rigid-limit values, that sets the limit on the rate of motion (15). On the basis of this shift in g_{xx}- and g_{yy}-values for position 8 in the lipid chain (Table 1), the rate of whole molecule lipid rotation must be slow, on the order of 10^7 s^{-1}. The Lorentzian half-width of the first-derivative $g_{xx}\text{-}g_{yy}$ averaged feature in the spectrum of 14-PCSL in hydrated Myr_2PtdCho/cholesterol is 1.85 mT, as opposed to 0.53 mT in the resolved part of the g_{yy} region of the rigid-limit spectrum. From this, it can be estimated (16) that the effective correlation time for rotation about the membrane normal is in the region of $\tau_{R//} \approx 1.5 \times 10^{-9}$ s or less, at the 14 position of the chain. [This is an upper estimate because it neglects contributions to the linewidth from off-axial motions (see below)]. The terminal methyl end of the chain is therefore undergoing pseudo-axial rotation on the nanosecond timescale in the cholesterol-containing systems, whereas the upper part of the chain (corresponding to the position of the steroid nucleus) remains fixed axially on this timescale.

Torsional flexing of the lipid chains is restricted in amplitude by the ordering effect of cholesterol, but is accompanied by line broadening in the g_{zz}-region of the spectrum. The Lorentzian half-widths of the three ^{14}N-hyperfine manifolds in this region of the spectrum are given as a function of the resonance position in Fig. 4. For the high-field hyperfine manifold, which displays the largest broadening and can be resolved best, the line broadening and shifts in the spectral positions are linearly related. Also, the shifts in line position are of the same order as the line broadening (see Fig. 4). These are characteristic features of slow Brownian rotational diffusion, as opposed to strong jump diffusion or fast motional averaging (5, 17). From the line broadening it is estimated that the effective rotational correlation time for the off-axis, chain-flexing motion ranges from the region of $\tau_{R\perp} \approx 1.5$ to 7.5×10^{-8} s for the 14-PCSL and 8-PCSL spin labels, respectively (18). Effective correlation times estimated from the line shifts are considerably shorter, which suggests that the motion is complex and that faster components are also involved, presumably those correlated with the axial rotation.

CONCLUSIONS

The high-frequency EPR results on spin-labeled lipid chains therefore demonstrate the simultaneous, off-axis, and non-axial ordering of the lipid chains by cholesterol in a liquid-ordered membrane phase. Axial averaging of the lateral chain orientation on the nanosecond timescale sets in first at the C-12 atom segment, which corresponds to the limit in transverse extent of the cholesterol steroid nucleus within the membrane. A great advantage of high-field EPR applied to spin labeling lies in the possibility to deduce the principal dynamic features of lateral and transverse ordering directly without resort to detailed spectral simulations (see refs. 5 and 6). This holds great promise for further spin-label applications to biological membranes and structural biology in general. In the present case, it is likely that the lateral lipid-chain ordering detected here contributes to the stabilization of cholesterol-rich, in-plane membrane domains, particularly of the detergent-resistant type, that are proposed to be involved in intracellular membrane sorting (19).

We thank Frau Brigitta Angerstein for technical assistance and synthesis of spin labels. This work was supported in part by National Institutes of Health Grant GM36232 (to B.J.G.).

1. McConnell, H. M. (1991) *Annu. Rev. Phys. Chem.* **42,** 171–195.
2. Recktenwald, D. J. & McConnell, H. M. (1981) *Biochemistry* **20,** 4505–4510.
3. Gaffney, B. J. & McConnell, H. M. (1974) *J. Magn. Reson.* **16,** 1–28.
4. Earle, K. A., Moscicki, J. K., Ge, M., Budil, D. E. & Freed, J. H. (1994) *Biophys. J.* **66,** 1213–1221.
5. Lebedev, Ya. S., Grinberg, O. Ya., Dubinsky, A. A. & Poluektov, O. G. (1992) in *Bioactive Spin Labels*, ed. Zhdanov, R. I. (Springer, Berlin), pp. 228–278.
6. Budil, D. E., Earle, K. A., Lynch, W. B. & Freed, J. H. (1989) in *Advanced EPR: Applications in Biology and Biochemistry*, ed. Hoff, A. J. (Elsevier, Amsterdam), pp. 307–340.
7. Vist, M. & Davis, J. H. (1990) *Biochemistry* **29,** 451–464.
8. Ipsen, J. H., Karlström, G., Mouritsen, O. G., Wennerström, H. & Zuckermann, M. J. (1987) *Biochim. Biophys. Acta* **905,** 162–172.
9. Brown, D. A. & London, E. (1997) *Biochem. Biophys. Res. Commun.* **240,** 1–7.
10. Harder, T. & Simons, K. (1997) *Curr. Opin. Cell Biol.* **9,** 534–542.
11. Marsh, D. & Watts, A. (1982) in *Lipid-Protein Interactions*, eds. Jost, P. C. & Griffith, O. H. (Wiley Interscience, New York), pp. 53–126.
12. Seddon, J. M., Templer, R. H., Warrender, N. A., Huang, Z., Cevc, G. & Marsh, D. (1997) *Biochim. Biophys. Acta* **1327,** 131–147.
13. Knoll, W., Schmidt, G., Ibel, K. & Sackmann, E. (1985) *Biochemistry* **24,** 5240–5246.
14. Finegold, L. & Singer, M. A. (1993) in *Cholesterol in Membrane Models*, ed. Finegold, L. (CRC, Boca Raton, FL), pp. 137–158.
15. Freed, J. H. (1976) in *Spin Labeling, Theory and Applications*, ed. Berliner, L. J. (Academic, New York), pp. 53–132.
16. Atherton, N. M. (1973) *Electron Spin Resonance. Theory and Applications* (Ellis Horwood, Chichester, U.K.).
17. Lebedev, Ya. S. (1994) in *Electron Spin Resonance, Vol. 14*, eds. Atherton, N. M., Davies, M. J. & Gilbert, B. C. (R. Soc. Chem., Cambridge, U.K.), pp. 63–87.
18. Lee, S. & Ames, D. P. (1984) *J. Chem. Phys.* **80,** 1766–1771.
19. Simons, K. & Ikonen, E. (1997) *Nature (London)* **387,** 569–572.